TECHNICAL RESEARCH REPORT

SYSTEMS RESEARCH CENTER

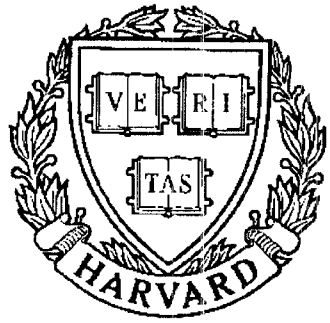

Supported by the National Science Foundation Engineering Research Center Program (NSFD CD 8803012), Industry and the University

Bifurcation Control of Chaotic Dynamical Systems

by H.O. Wang and E.H. Abed

TR 92-67

Bifurcation Control of Chaotic Dynamical Systems*

Hua O. Wang and Eyad H. Abed

Department of Electrical Engineering

and the Institute for Systems Research

University of Maryland, College Park, MD 20742 USA

Manuscript: June 6, 1992

Abstract

A nonlinear system which exhibits bifurcations, transient chaos, and fully developed chaos is considered, with the goal of illustrating the role of two ideas in the control of chaotic dynamical systems. The first of these ideas is the need for *robust control*, in the sense that, even with an uncertain dynamic model of the system, the design ensures stabilization without at the same time changing the underlying equilibrium structure of the system. Secondly, the paper shows how focusing on the control of primary bifurcations in the model can result in the taming of chaos. The latter is an example of the 'bifurcation control' approach. When employed along with a dynamic feedback approach to the equilibrium structure preservation issue noted above, this results in a family of robust feedback controllers by which one can achieve various types of 'stability' for the system.

Keywords: Chaos, dynamical systems, bifurcation, feedback, control.

*Based on a paper to be presented at the Second IFAC Nonlinear Control Symposium, Bordeaux, France, June 24-26,1992.

1 Introduction

Recently, significant attention has been focused on developing techniques for the control of chaotic dynamical systems [1,2,3,4,5,6]. Of course, at the outset, one must realize that there is no obvious way to define the 'control of chaos' problem. This is in direct contrast to more traditional dynamical system control problems, such as the textbook problem of stabilization of an equilibrium position of a nonlinear system. Although even this textbook problem allows for various interpretations for the achieved margin of stability, decay rate, etc., these can all be viewed within the same basic framework. Chaos, on the other hand, is a rich, global dynamic behavior, and its 'stabilization' can have vastly differing interpretations. For example, references [2,3] employ a small amplitude control law in a restricted region of the state space, thereby stabilizing a pre-existing equilibrium or periodic orbit. Since the control vanishes in most of the state space, closed-loop system trajectories follow erratic paths for some time, until they enter part of the neighborhood in which the control is effective, after which they are attracted to the equilibrium or periodic orbit of interest. Other authors apply nonlocal linear or nonlinear feedback to stabilize nominal equilibrium points [1,5]. Also, some authors are taking a control systems approach to the analysis of chaos, which may prove useful in control design (see [7,8,9]). This summary of previous work on control of chaos is of necessity very brief, and the reader is referred to the original papers for details.

In general, the techniques for feedback control of chaos presented thus far in the literature have some common features, which we feel are important to briefly summarize. The control is usually designed for parameter values where the system is known to exhibit chaotic motion, and is typically of the form $u = u(x - x_0)$ where x is the system state vector, and x_0 is an unstable equilibrium of interest, which lies on a chaotic attractor. The control function u is not necessarily smooth. Thus, the control consists of direct state (or output) feedback around x_0, a specific equilibrium of interest. Note that x_0 can also be a periodic orbit, as observed in [2,3].

The approach pursued in the present paper is directed toward nonlinear systems which undergo bifurcations, and possibly chaotic motion, as a parameter is quasistatically varied.

Such systems naturally possess several, and possibly infinitely many, equilibria and periodic orbits. The approach is of particular relevance to systems for which the model possesses a high degree of uncertainty. Often, an engineering system is designed to perform well, and to be stable, for a large range of parameter values. However, technological demands are pushing systems to the limits of their performance, and many engineering systems are being operated under conditions which may be viewed as 'stressed.' It is this stressed operation which gives rise to nonlinear dynamic phenomena, such as bifurcations leading, in some cases, to chaos. We take an approach which is in mathematical synergy with this description.

We consider nonlinear systems depending, for simplicity, on a single bifurcation parameter. For the 'usual' values of the parameter, the system operates at a stable equilibrium, and perturbations away from this mode of operation tend to be attenuated (stability). As the parameter is varied, the equilibrium loses stability at a bifurcation point, giving rise to new equilibria or periodic orbits, perhaps. If any of the bifurcated solutions is stable, the system may operate at such a solution. For greater variations of the parameter, these bifurcated solutions may also lose stability, and so on. There are several scenarios by which successive bifurcations can result in a chaotic invariant set; these are discussed extensively in the chaos literature. What is important about these scenarios from a control of chaos perspective, however, is that the appearance of chaos depends heavily on various aspects of the succession of bifurcations. Suppose a particular control significantly reduces the amplitude of a bifurcated solution, or significantly enhances its stability, over a nontrivial parameter range. Then, one might expect that the occurrence of chaos might be 'delayed' to even greater variations in the parameter, or might be extinguished completely.

This work differs from previous techniques in another respect, related to nonlinear model uncertainty. Under model uncertainty, a nonlinear static state feedback controller designed relative to a given equilibrium will influence not only the stability, but also the location, of this and other system equilibria. To circumvent this difficulty, we employ a form of dynamic feedback which exactly preserves all system equilibria. This uses washout filters in a way which retains sufficient freedom to stabilize bifurcations, and to delay their occurrence if

desired (see [10]). Besides preserving system equilibria, the incorporation of washout filters in the feedback control facilitates the design of a control which does not depend on the bifurcation parameter. This is also important to achieving a control which is effective over a range of parameter values, instead of at one specific parameter value.

In this paper, we focus on a system studied by Singer, Wang and Bau [1] as a vehicle for illustrating the bifurcation control approach. Singer, Wang and Bau study control of a thermal convection loop using an experimental apparatus, and compare their experimental results with simulations based on a low order dynamic model. The model is related to the Lorenz equations [11]; see, e.g., Jackson [12] for a derivation. In [1] simple control laws are given which suppress chaos in the model and in the experimental apparatus. Two more recent papers by Bau and coworkers addressing control of chaos are [13], [14].

As stated in the foregoing comments, the bifurcation control approach to control of chaos will be employed in the present paper. For the convective loop model used in [1], the results obtained below provide a systematic alternative to construction of control laws. Moreover, the controlled system possesses the desirable properties discussed above.

The remainder of the paper is organized as follows. Section 2 reviews the thermal convection loop model of [1], and discusses its open loop dynamical behavior. Section 3 provides a brief summary of concepts and results from [10,15,16] on bifurcation control. Section 4 applies these results to the thermal convection loop model to determine control laws for suppressing both the transient chaotic and chaotic motion of the thermal convection loop model. Concluding remarks are given in Section 5.

2 Thermal Convection Loop Model

Singer, Wang and Bau [1] study a thermal convection loop using a combination of experimentation, modeling, and simulation. The analytical model used in [1] is given by the third order system

$$\dot{x}_1 = -px_1 + px_2, \tag{1}$$

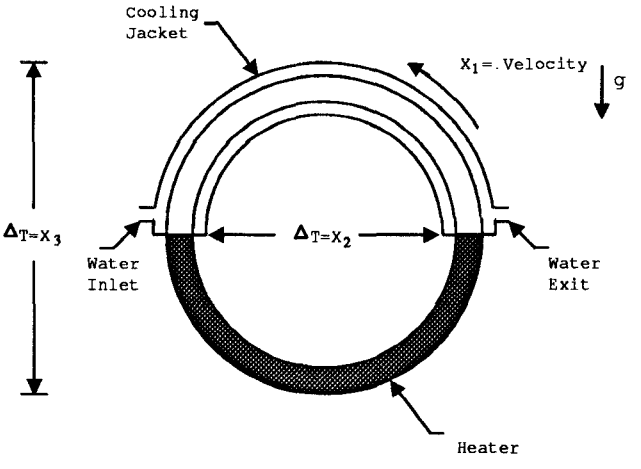

Figure 1: Schematic description of the experimental apparatus

$$\dot{x}_2 = -x_1 x_3 - x_2, \tag{2}$$

$$\dot{x}_3 = x_1 x_2 - x_3 - R. \tag{3}$$

where $x_i, i = 1, 2, 3$, are real, and p and R are positive parameters. The experiment studied in [1] involves thermal convection in a toroidal vertical loop heated from below and cooled from above as depicted in Figure 1. The variables x_1, x_2, x_3 correspond, respectively, to the cross-sectionally averaged velocity in the loop, the temperature difference along the horizontal direction (side to side), and the temperature difference along the vertical direction (top to bottom). The parameter R is the Rayleigh number, which is proportional to the net heating rate, and p denotes the Prandtl number. It is observed experimentally that, as the heating rate increases, the fluid flow in the loop goes through transitions. For a low heating rate, the fluid is in the no-motion state. As the heating rate increases, a state of steady convection arises (clockwise or counterclockwise). Further increases in the heating rate result in temporally oscillatory, and, eventually, chaotic motion of the fluid.

The transitions above are also reflected by the model (1)-(3). To facilitate discussion of this model, set $p = 4.0$ and view R as the bifurcation parameter. A bifurcation diagram related to this model is given in Figure 2. In this diagram, a solid line represents a stable equilibrium, a dashed line represents an unstable equilibrium, and an open circle represents the maximum amplitude of an unstable periodic orbit of (1)-(3). The bifurcation diagram

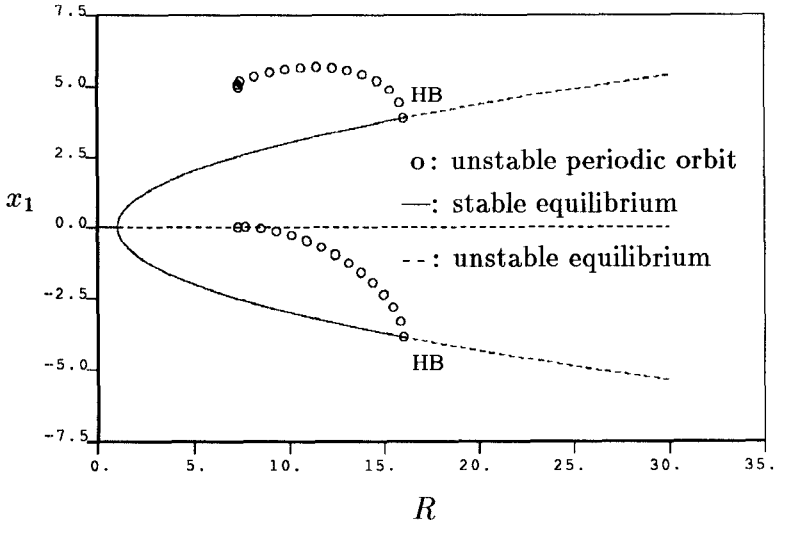

Figure 2: Bifurcation diagram for open loop system

is obtained by employing the package AUTO [17]. The model (1)-(3) possesses symmetry, in that replacing (x_1, x_2, x_3) with $(-x_1, -x_2, x_3)$ results in the same set of equations. This symmetry is reflected in the bifurcation diagram of Fig. 2.

For $R \leq 1.0$ the system (1)-(3) has a single, globally attracting, equilibrium point. This equilibrium, given by $x_1 = x_2 = 0, x_3 = -R$, corresponds to the *no-motion state*. At $R = 1.0$ two additional equilibrium points appear through a pitchfork bifurcation. These equilibria, which are present for all $R > 1.0$, are given by $(x_1 = x_2 = \pm\sqrt{R-1}, x_3 = -1.0)$. Denote these equilibria by C_+ and C_-, respectively. These two equilibrium points represent the states of steady convection in the counterclockwise or clockwise directions, respectively. The no-motion equilibrium state $(0, 0, -R)$ loses its stability at the pitchfork bifurcation point, i.e., at $R = 1.0$. The convective equilibria $(\pm\sqrt{R-1}, \pm\sqrt{R-1}, -1.0)$ lose their stability in Hopf bifurcations occurring at $R = p(p+4)/(p-2) = 16.0$, as depicted in Fig. 2. The bifurcation diagram of Fig. 2 illustrates that the Hopf bifurcations at the convective equilibria result in *unstable* periodic solutions, i.e., these bifurcations are subcritical. Moreover, Fig. 2 also illustrates the disappearance of the unstable periodic orbit in a blue sky catastrophe [18] at the approximate value $R = 7.3198$. Not discernible from Fig. 2 is the fact that the model (1)-(3) admits erratic behavior for a large range of values of R. This erratic behavior

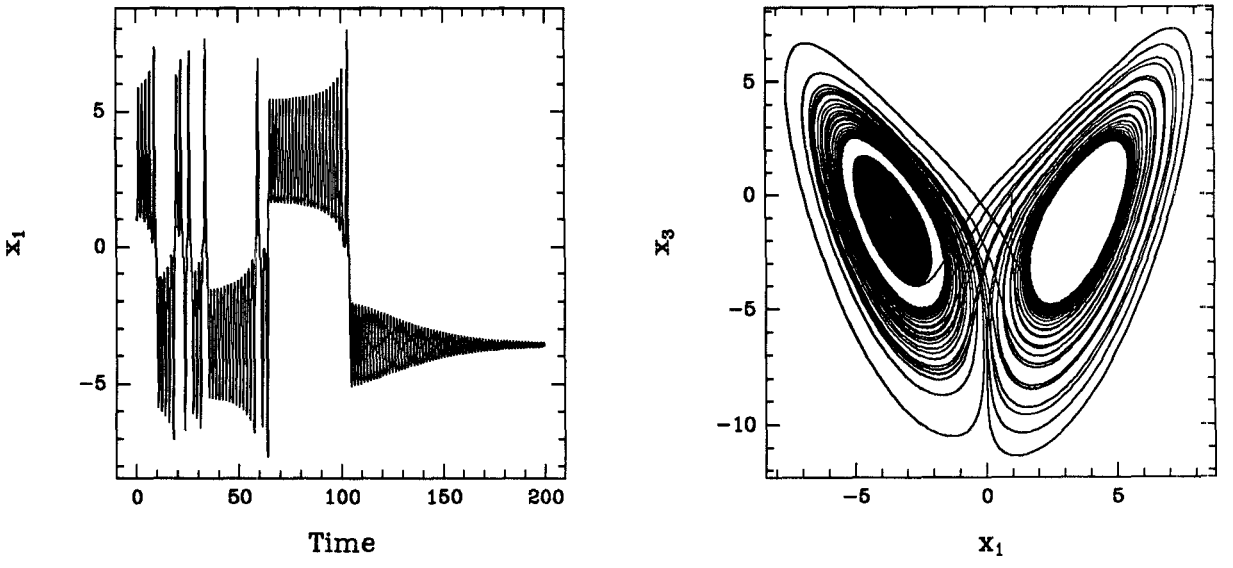

(a) (b)

Figure 3: A transient chaotic orbit of open loop system for $R = 14$

may or may not be chaotic. To be more precise, one observes trajectories which appear chaotic for a long time interval, after which they settle to an equilibrium. One also observes trajectories which are chaotic in the usual sense. The former type of behavior is often referred to as "transient chaos." Transient chaos is observed in simulations of (1)-(3) for parameter values $7.3198 < R < 15.9$, for *some* initial conditions. (Extensive simulation shows that initial conditions resulting in transient chaos are more common for larger values of R in this interval. See Figure 3 for a typical transient chaotic trajectory of the system at $R = 14$.) At approximately $R = 15.9$ the transient chaos is converted to a chaotic attractor by a crisis. Thus for the relatively narrow range $15.9 < R < 16$, there are three possible attractors, namely C_+, C_- and a chaotic attractor, while for $R > 16$, typical trajectories of the system (1)-(3) are chaotic. Figure 4 shows a typical chaotic trajectory of the system at $R = 19$.

The foregoing is a necessarily brief description of the qualitative behavior of (1)-(3) and its dependence on the parameter R. There are, however, intricate details associated with the various behaviors and their bifurcations. For instance, there are several stable periodic

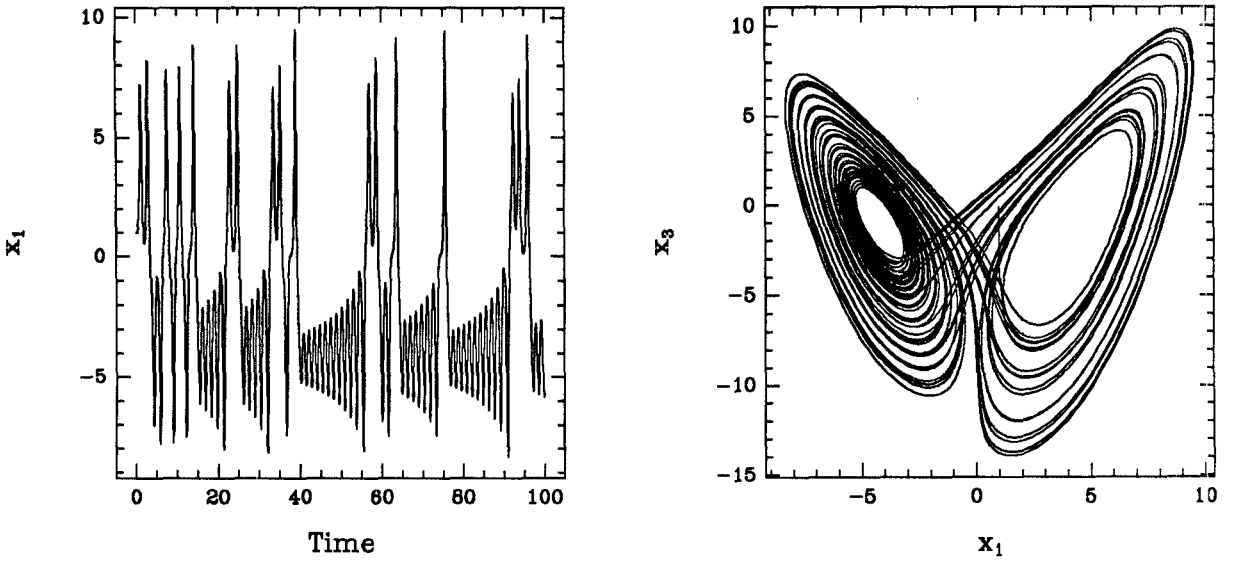

Figure 4: A chaotic orbit of open loop system for $R = 19$

orbit windows for some large values of R. Within these windows there are three kinds of bifurcations involving periodic orbits, namely, the saddle-node bifurcation, the symmetry breaking bifurcation and the period doubling bifurcation [11]. The most noticeable periodic orbit window corresponds roughly to the parameter range $125 < R < \infty$.

Not only do Eqs. (1)-(3) resemble the Lorenz equations, but there is a simple transformation mapping the Lorenz system into (1)-(3). The Lorenz equations are

$$\dot{x} = -\sigma x + \sigma y, \tag{4}$$

$$\dot{y} = rx - y - xz, \tag{5}$$

$$\dot{z} = xy - bz, \tag{6}$$

where σ, r and b are three positive parameters. Equations (1)-(3) can be obtained from the Lorenz equations by the transformation

$$x_1 = x, \tag{7}$$

$$x_2 = y, \tag{8}$$

$$x_3 = z - r, \tag{9}$$

with the identifications $R = r, p = \sigma$ and $b = 1$. Hence, studies of the Lorenz equations have a direct bearing on the system (1)-(3). We should note that the homoclinic orbits at $R = 7.3198$, which may be viewed as being 'caused' by the subcriticality of the Hopf bifurcations, are important to the appearance of the transient chaotic and chaotic motions of the model studied here. Indeed, the transient chaos occurring near the homoclinic bifurcation results from a Sil'nikov-type bifurcation [19], [11]. (The model also exhibits chaotic behavior in other, distant parameter ranges arising from period doubling cascades.) Before pursuing the design of feedback control laws for the system above, it is necessary to briefly summarize results on bifurcation control.

3 Bifurcation Control Laws

Consider a one-parameter family of nonlinear autonomous control systems

$$\dot{x} = f_\mu(x, u). \tag{10}$$

where $x \in \mathbb{R}^n$ is the state vector, $\mu \in \mathbb{R}$ is the system parameter, f_μ is a smooth map from $\mathbb{R}^n \times \mathbb{R}$ to $\mathbb{R}^n$ and u is a scalar input. Local bifurcation control deals with the design of smooth control laws $u = u(x)$ which stabilize a bifurcation occurring in the one-parameter family of systems (10). These control laws exist generically, even if the critical eigenvalues of the linearized system at the equilibrium of interest are uncontrollable. The direct state feedback control designs of [15] result in transforming a subcritical (unstable) Hopf bifurcation to a supercritical, and hence stable, bifurcation. This was extended to stabilization of Hopf bifurcations using dynamic feedback through washout filters in [10, 16]. The washout filter-aided feedback control law developed in [10,16] has many desirable features. The control law does not require an accurate knowledge of the system equilibria and it exactly preserves all system equilibria. Also the incorporation of washout filters in the feedback control facilitates the design of a control which does not depend on the

bifurcation parameter. This is important to achieving a control which is effective over a range of parameter values.

The design procedure aims to ensure the asymptotic stability of the Hopf bifurcation point as well as orbital asymptotic stability of the periodic solutions emerging from the bifurcation point for a range of parameter values. Suppose for $u = 0$, x_{e,μ_c} is the nominal equilibrium of (10) with $\mu = \mu_c$ and the following hypothesis (hypothesis(H)) holds: The Jacobian matrix $D_x f_{\mu_c}(x_{e,\mu_c}, 0)$ has a simple pair of nonzero pure imaginary eigenvalues $\lambda_1(\mu_c) = j\omega_c$ and $\lambda_2(\mu_c) = -j\omega_c$ with $\omega_c \neq 0$ and the transversality condition

$$\frac{\partial Re[\lambda(\mu_c)]}{\partial \mu} \neq 0 \tag{11}$$

is satisfied, and all the remaining eigenvalues are in the open left half complex plane. The Hopf Bifurcation Theorem [20], [21] asserts the existence of a one-parameter family $p_\epsilon, 0 < \epsilon \leq \epsilon_0$ of nonconstant periodic solutions of system (10) emerging from $x = x_{e,\mu_c}$ at the parameter value μ_c for ϵ_0 sufficiently small. The periodic solution $p_\epsilon(t)$ occurring at parameter values $\mu(\epsilon)$ have period near $2\pi\omega_c{}^{-1}$. Exactly one of the characteristic exponents of p_ϵ governs the asymptotic stability and is given by a real, smooth and even function

$$\beta(\epsilon) = \beta_2\epsilon^2 + \beta_4\epsilon^4 + \cdots. \tag{12}$$

That is, p_ϵ is orbitally asymptotically stable if $\beta(\epsilon) < 0$ but is unstable if $\beta(\epsilon) > 0$. Generically the local stability of the bifurcated periodic solutions p_ϵ is typically decided by the sign of the coefficient β_2. Note the sign of β_2 also determines the stability of the critical equilibrium point x_{e,μ_c}. Therefore, a feedback control law $u = u(x)$ which renders $\beta_2 < 0$ will stabilize both the Hopf bifurcation point and the bifurcated periodic solutions.

There are several concerns about this form of control function u. Usually the argument of u is $\hat{x} = x - x_{e,\mu_c}$, but this limits the control to one parameter value μ_c since $f_\mu(x_{e,\mu}, u(x - x_{e,\mu_c}))$ does not necessarily vanish for $\mu \neq \mu_c$. Here $x_{e,\mu}$ is an equilibrium point of $f_\mu(x_{e,\mu}, 0)$. Another option is to take the argument of the control function to be $\hat{x}_\mu = x - x_{e,\mu}$. Clearly this requires knowledge of the whole branch of equilibria within the neighborhood of x_{e,μ_c} of interest and more severely requires the control u to depend on the parameter μ. Even

if $x_{e,\mu}$ can be determined accurately, if the system has multiple equilibrium branches, i.e., there is at least one equilibrium point $x'_{e,\mu} \neq x_{e,\mu}$, the control above still does not preserve other branches like $x'_{e,\mu}$. These concerns lead to the employment of the outputs of washout filters as the arguments to the control u in [10].

Specifically, in Eq. (10), for each system state variable x_i, $i = 1, \ldots, n$, introduce a washout filter governed by the dynamic equation

$$\dot{z}_i = x_i - d_i z_i \tag{13}$$

along with output equation

$$y_i = x_i - d_i z_i. \tag{14}$$

Here, the d_i are positive parameters (this corresponds to using stable washout filters). In this formulation, n washout filters, one for each system state, are present. In fact, the actual number of washout filters needed, and hence also the resulting increase in system order, can usually be taken less than n.

The advantages of using washout filters in this way stem from the resulting properties of equilibrium preservation and automatic equilibrium (operating point) following. For instance, if $u = u(y)$ with $u(0) = 0$ where y is a washout filter output (14), clearly y vanishes at steady-state. Hence the x components of a closed loop equilibrium are identical with the corresponding components of the open loop equilibrium. Also, since Eq. (14) can always be written as

$$y_i = x_i - dz_i = (x_i - x_{i_{e,\mu}}) - d(z_i - z_{i_{e,\mu}}), \tag{15}$$

the control function $u = u(y)$ is guaranteed to center at the correct operating point. Moreover it is shown in [16] that, at a Hopf bifurcation point, the extended system (10) and (13) has the same stability coefficient β_2 as that of the original system (10).

It is well known that only the quadratic and cubic terms occurring in a nonlinear system undergoing a Hopf bifurcation influence the value of β_2. Thus only the linear, quadratic and cubic terms in an applied control u have potential for influencing β_2. Now assume any linear feedback, which may be used to modify the critical parameter value μ_c, is reflected in the

nominal system (10) and (13). Then the feedback control u may be assumed to be of the form

$$u = y^T Q_u y + C_u(y, y, y), \tag{16}$$

where y is the vector of washout filter outputs $y_i = x_i - d_i z_i$, Q_u is a real symmetric $n \times n$ matrix and C_u is a cubic form generated by a scalar-valued symmetric trilinear form. Such a control law is independent of the equilibrium points, and, because of its nonlinearity, preserves the linear stability characteristics of the original system.

Due to space limitations, we only briefly summarize the results for the situation that the critical eigenvalues of the linearized system at the equilibrium of interest are controllable, which is the case of the convection loop dynamics. The Taylor series expansion of (10) with respect to x and u at $x = x_{e,\mu_c}, u = 0$ gives

$$\dot{\hat{x}} = A_0 \hat{x} + bu + \cdots. \tag{17}$$

where $\hat{x} := x - x_{e,\mu_c}$. Let r be the right (column) and l the left (row) eigenvector of A_0 with eigenvalue $j\omega_c$. Normalize by setting the first component of r to 1 and then choose l so that $lr = 1$. From the well known PBH test[22], controllability of the critical mode is equivalent to the requirement $lb \neq 0$. In such case a linear stabilizing feedback exists. Interestingly it is shown in [15,16] that a cubic stabilization feedback also exists. That is Q_u can be set to 0 in Eq. (16). For simplicity, let the washout filter parameters d_i all be given by a common value, say $d > 0$. The closed-loop stability coefficient β_2^* of the overall system (10), (13), (14) and (16) (with $Q_u = 0$) is given by [16]:

$$\beta_2^* = \beta_2 + 2Re\Delta, \tag{18}$$

where β_2 is the stability coefficient of the original system (10) or the extended system (10), (13) and Δ is given by

$$\Delta = \frac{3}{4} \frac{\omega_c^3(\omega_c + jd)}{(d^2 + \omega_c^2)^2} C_u(r, r, \bar{r}) lb. \tag{19}$$

where r, l, b, d and ω_c are from above. From this we see the control can be any cubic function $C_u(y, y, y)$ such as $Re\Delta$ is sufficiently negative to ensure $\beta_2^* < 0$. Such control stabilizes the

Hopf bifurcation point and the periodic solutions emerging from the Hopf bifurcation point for a range of parameter values.

4 Bifurcation Control of Convection Dynamics

In this section, we employ the bifurcation control results above to determine control laws for suppressing both the transient chaotic and chaotic motion of the system (1)-(3). In the course of seeking control laws for suppression of chaos, we shall also employ feedback to achieve other, subsidiary goals. For instance, in the next subsection we consider use of feedback to delay to higher values of the Rayleigh number the occurrence of the Hopf bifurcations from the convective equilibria $C_{\pm}$. This addresses a question which arises rather naturally in the context of using feedback to modify the phase portrait of system (1)-(3) in useful ways. The control laws developed for achieving this delay in Hopf bifurcation parameter values have a feature which occurs throughout this paper: *they do not result in any change in the set of equilibria, even in the presence of model uncertainty.* This is achieved using dynamic feedback incorporating washout filters, as proposed in [10,16].

4.1 Delaying the Hopf Bifurcations

Recall that the convective equilibria $C_{\pm}$ lose their stability at Hopf bifurcations occurring at $R = 16$. In this subsection, we give controllers which result in changing this critical value of R to some prescribed value. In practice, the prescribed value would likely be greater than the nominal (open loop) value, so as to result in an increase in the range of parameter values for which the system exhibits stable steady motion.

Linearizing the model (1)-(3) at the upper equilibrium C_+ of Fig. 2, we find that, for $R = 16$, the Jacobian matrix has a pair of imaginary eigenvalues $\pm i\omega_c$ where $\omega_c = 4.47214$ (recall that $p = 4$). Next we present a feedback control scheme which allows one to modify the critical value of R at which the Hopf bifurcations occur, and to do so without modifying the equilibria of (1)-(3). The state variable x_3 is readily observable.

A *linear washout filter aided feedback* with measurement of x_3 is a dynamic feedback described as follows. The closed loop system is given by

$$\dot{x}_1 = -px_1 + px_2, \tag{20}$$

$$\dot{x}_2 = -x_1x_3 - x_2, \tag{21}$$

$$\dot{x}_3 = x_1x_2 - x_3 - R + u, \tag{22}$$

$$\dot{x}_4 = x_3 - dx_4, \tag{23}$$

where x_4 is the washout filter state, and where the control u is of the form

$$u = -k_l y, \tag{24}$$

with y an output variable, given by

$$y := x_3 - dx_4. \tag{25}$$

Here, k_l is a scalar (linear) feedback gain.

This control preserves the symmetry inherent in the model (1)-(3). Thus, in discussing the effects of the controller above, remarks specific to the upper equilibrium branch C_+ apply also to the lower branch C_-.

The control above is a dynamic feedback control. By adjusting the linear control gain k_l one can delay the Hopf bifurcations to occur at any desired parameter value. The relationship between the critical parameter value R and the control gain k_l can be determined by finding the conditions under which the Jacobian of the overall system (20) - (25) possesses a pair of pure imaginary eigenvalues. This relationship translates to the conditions

$$\begin{aligned}
&(Rd - 2p + 2Rp + dp)^2 \\
&+ (2 + d + k_l + p)^2(-2dp + 2Rdp) \\
&- (2 + d + k_l + p)(Rd - 2p + 2Rp \\
&+ dp)(R + 2d + k_l + p + dp + k_l p) = 0,
\end{aligned} \tag{26}$$

$$k_l + p + d + 2 > 0, \text{ and } R > 1 \tag{27}$$

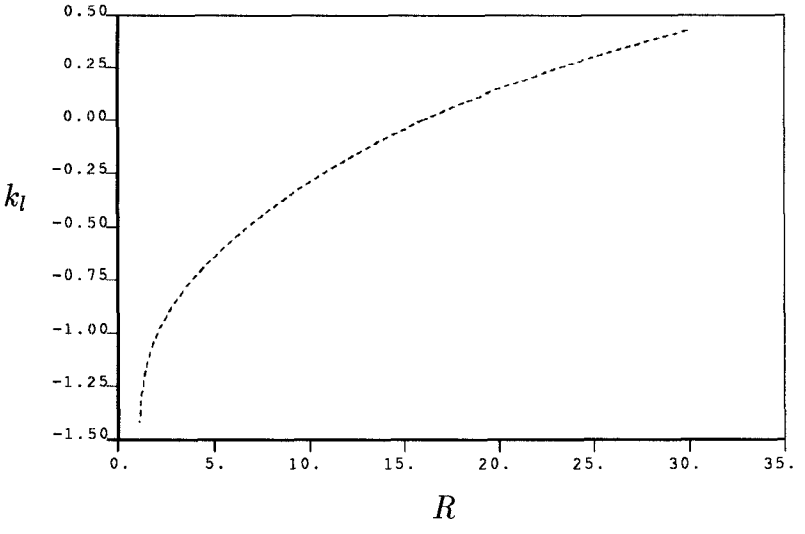

Figure 5: Two-parameter curve of Hopf bifurcation points for linear 'delaying' control

In the case $p = 4.0$ and $d = 0.5$, these conditions are tantamount to the restriction

$$-1.5 < k_l < 2 \tag{28}$$

on the gain k_l. To *delay* occurrence of the Hopf bifurcations, however, one must further restrict k_l to be positive. Indeed, negative values of k_l in the interval $-1.5 < k_l < 2$ result in moving the Hopf bifurcations to smaller values of R. Figure 5 shows the 2-parameter (k_l and R) curve of the Hopf bifurcation points, i.e., the relationship between k_l and critical parameter value R. Figures 6(a) and 6(b) depict the bifurcation diagrams for the closed loop system with (a) $k_l = 0.182538$ and (b) $k_l = -0.234191$, respectively. In Figure 6(a), the Hopf bifurcations are delayed to $R = 21$, while in Figure 6(b), the Hopf bifurcations are moved ahead to $R = 11$.

The foregoing discussion has resulted in linear, dynamic feedback control laws which can be tuned to result in moving the Hopf bifurcation points to any desired value of $R > 1$. These control laws also ensure asymptotic stability of the convective equilibria for all values of R up to the desired critical value. Despite this positive conclusion, the closed loop system incorporating the control laws given above still exhibits chaotic and transient chaotic behavior. This chaotic behavior is delayed to greater values of R if $0 < k_l < 2$, and moved

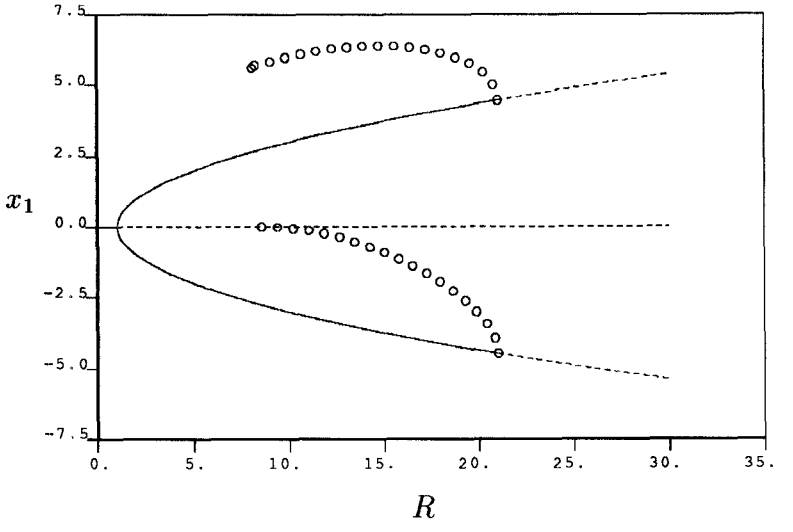

(a)

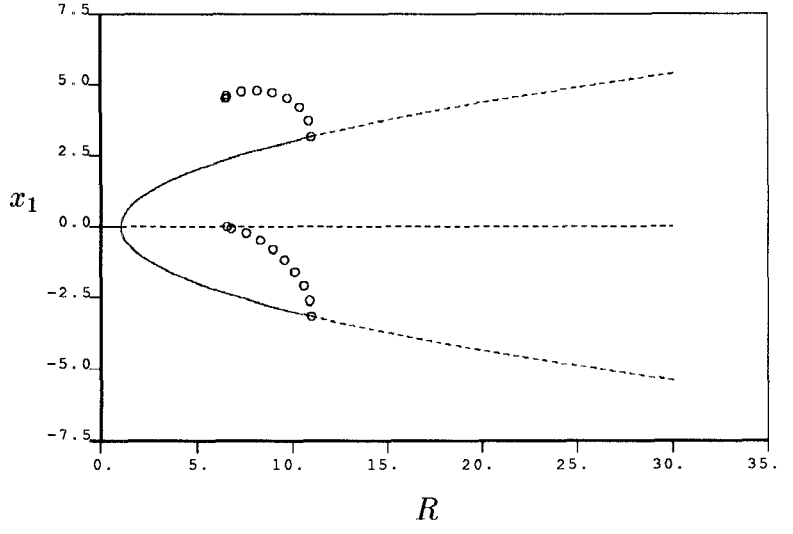

(b)

Figure 6: Bifurcation diagrams for linear 'delaying' control with (a) $k_l = 0.182538$ (b) $k_l = -0.234191$

ahead to lesser values if $-1.5 < k_l < 0$.

From the discussion above it is clear that linear feedback can stabilize the convective equilibria for arbitrary ranges of the parameter. Also as shown below, further increases in the control gain result in the annihilation of the Hopf bifurcations. These, however, do not imply that such a feedback can suppress chaos in the system. The transient chaos and chaos which occur due to the presence of homoclinic orbits in the open loop system can be suppressed by this type of linear dynamic feedback with a higher feedback gain. Specifically, for gains $k_l > 2$ and for $p = 4, d = 0.5$, it can be shown that both the upper and lower convective equilibria are rendered asymptotically stable, and that the system no longer exhibits chaos or transient chaos that arise through the homoclinic orbits and loss of stability of the convective equilibria. However, the chaotic motion in the open loop system which results from period doubling cascades persists for the closed loop system with linear feedback. Moreover, for large values of R (e.g. $R > 275$), besides the two stable convective equilibria as attractors, there are large amplitude stable period orbits.

We proceed to investigate two alternatives to linear feedback of the type considered above. First, a nonlinear feedback control law can be designed to stabilize the Hopf bifurcations and introduce a small amplitude stable limit cycle which surrounds the equilibrium for parameter values at which it is unstable. Second, one can employ a combined linear-plus-nonlinear feedback to suppress chaos in the closed loop system. The linear part of the feedback is tuned to delay the Hopf bifurcations to a desired value of R, and the nonlinear part of the feedback is chosen to stabilize the Hopf bifurcations occurring in the closed loop system. The linear-plus-nonlinear feedback control alternative is the more versatile of these.

Before proceeding to issues of nonlinear control design, we remark that the control introduced in the foregoing does not affect the stability of the nominal equilibrium branch, $(0, 0, -R, -R/d)$. This is easy to prove by examining the associated characteristic polynomial

$$\begin{aligned} D_0(s) &= s^4 + (2 + d + k_l + p)s^3 + (1 + 2d + k_l + 2p + dp + k_l p - pR)s^2 \\ &\quad + (d + p + 2dp + k_l p - pR - dpR - k_l pR)s + dp - dpR. \end{aligned} \tag{29}$$

Clearly for $R \geq 1$, $D_0(s)$ is not a Hurwitz polynomial, i.e., $(0, 0, -R, -R/d)$ is unstable for $R \geq 1$. This is the same as in the open loop case.

4.2 Stabilizing the Hopf Bifurcations

Suppose a dynamic linear feedback has been introduced as in the foregoing subsection, resulting in positioning the Hopf bifurcations to a desired value of R. One result of such a control is to affect the bifurcated periodic solutions which emerge at the two Hopf bifurcations. Recall that these bifurcations are subcritical for the open loop system (see Fig. 2). The subcriticality of the Hopf bifurcations is crucial to the appearance of transient chaos and chaos in the model for various values of R. Thus the question arises as to whether or not the feedback controller of the previous subsection can be modified to result in stabilization of the Hopf bifurcations. Next, we summarize some positive results in this direction.

From formulae (18) and (19) it can be seen that any cubic function $C_u(y, y, y)$ such that $Re\triangle$ is sufficiently negative to ensure $\beta_2^* < 0$ will serve to stabilize the Hopf bifurcations. In other words, there is a family of stabilizing, purely cubic nonlinear controllers. We now choose the simplest such stabilizing control law. The closed loop system again takes the form (20)-(25), except that now the controller is

$$u = -k_n y^3. \tag{30}$$

Here, k_n is the nonlinear feedback gain.

Again this control preserves the symmetry inherent in the model (1)-(3). Thus, in discussing the effects of the controller above, remarks specific to the Hopf bifurcation associated with the upper equilibrium branch C_+ apply also to that of the lower branch C_-.

To illustrate the utility of such a nonlinear control law, we state a simple result obtained using formulae (18) and (19) for β_2^* in the case $p = 4.0$ and $d = 0.5$:

$$\beta_2^* = \beta_2 - 2.42505 k_n. \tag{31}$$

The open loop quantity β_2 can be computed using either a known algorithm (e.g., [15]) or the software package BIFOR2 [20]. Using BIFOR2 we obtain $\beta_2 = 0.02027 \pm 0.001087$. Thus,

any choice of control law (30) with $k_n > 0.009$ stabilizes the Hopf bifurcations occurring at $R = 16$. This is a local result. To assess the degree to which this is reflected in the global dynamics of the system, one resorts to extensive computation. Figure 7 shows the bifurcation diagram for the closed loop system with $k_n = 0.009$. Solid circles indicate stable limit cycles. The maximum amplitude of a stable limit cycle is given by a solid circle. The periodic orbits emerging from the Hopf bifurcation points themselves undergo further bifurcations. In the closed loop system, the stable periodic orbits emerging from the Hopf bifurcation points lose stability through cyclic fold bifurcations (CFB) [18]. The resulting unstable periodic orbits regain their stability at the secondary Hopf bifurcations (or Hopf bifurcations involving periodic orbits). In the interval between the cyclic fold and secondary Hopf bifurcations, the Ruelle-Takens route to chaos from the secondary Hopf bifurcations takes place. Simulations suggest that for $k_n = 0.009$, this interval in parameter space is the only range of parameter values where chaos is present. Simulations along with application of the bifurcation analysis tool AUTO [17] indicate that slightly larger values of the gain k_n result not only in annihilation of the Ruelle-Takens route to chaos, but also in a reduced amplitude of the stable limit cycles. This is illustrated in Figure 8, which shows superimposed bifurcation diagrams for the closed loop system with various control gains k_n. Figure 9 shows a typical system trajectory for the closed-loop system with $k_n = 2.5$ at $R = 19$.

With this type of control, transient chaos is successfully suppressed, and the previous chaotic trajectories are replaced by small amplitude stable limit cycles near the convective equilibria. Moreover, extensive simulations demonstrate that the periodic orbit windows cease to exist, as does the chaos arising from the period doubling bifurcations associated with these windows.

We conclude this subsection with a few comments on the Ruelle-Takens route to chaos and our proposed control. By taking the control gain k_n near 0.009, we in fact transfer the chaos scenario associated with the original system to a new one, namely, the Ruelle-Takens route to chaos. More significantly, slight increases in k_n result in annihilation of this route to chaos. Thus, the proposed control may also be a candidate for the control of the

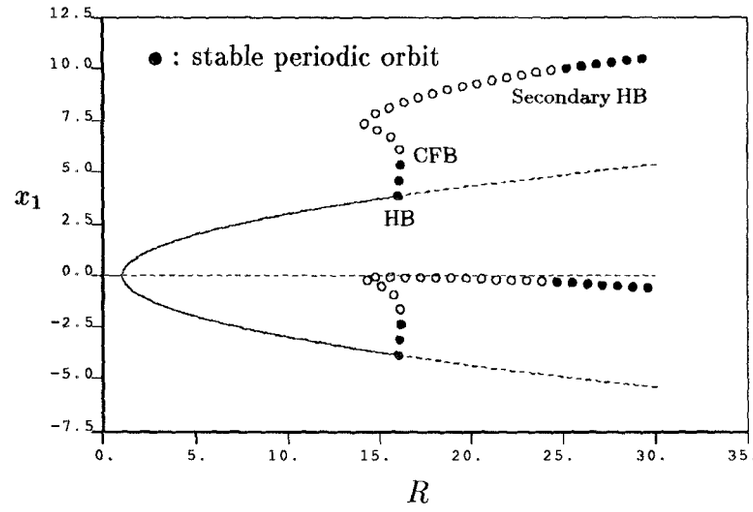

Figure 7: Bifurcation diagram for nonlinear 'stabilizing' control with $k_n = 0.009$

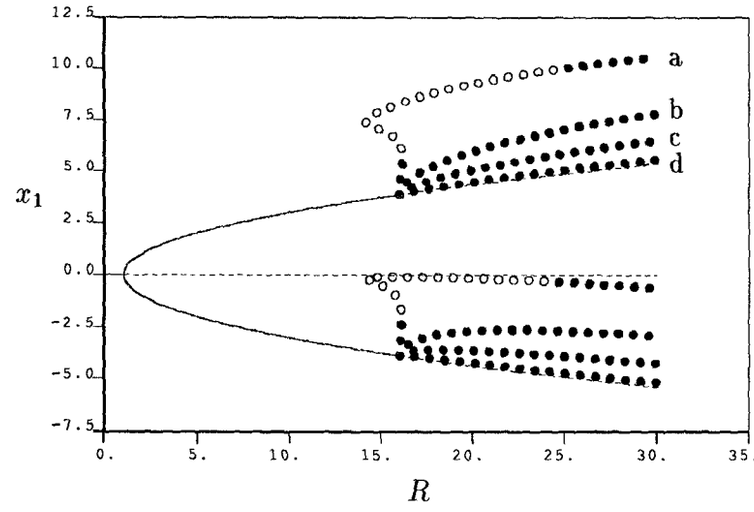

Figure 8: Superposed bifurcation diagrams for nonlinear 'stabilizing' control with different control gains k_n: a. 0.009, b. 0.025, c. 0.1, d. 2.5

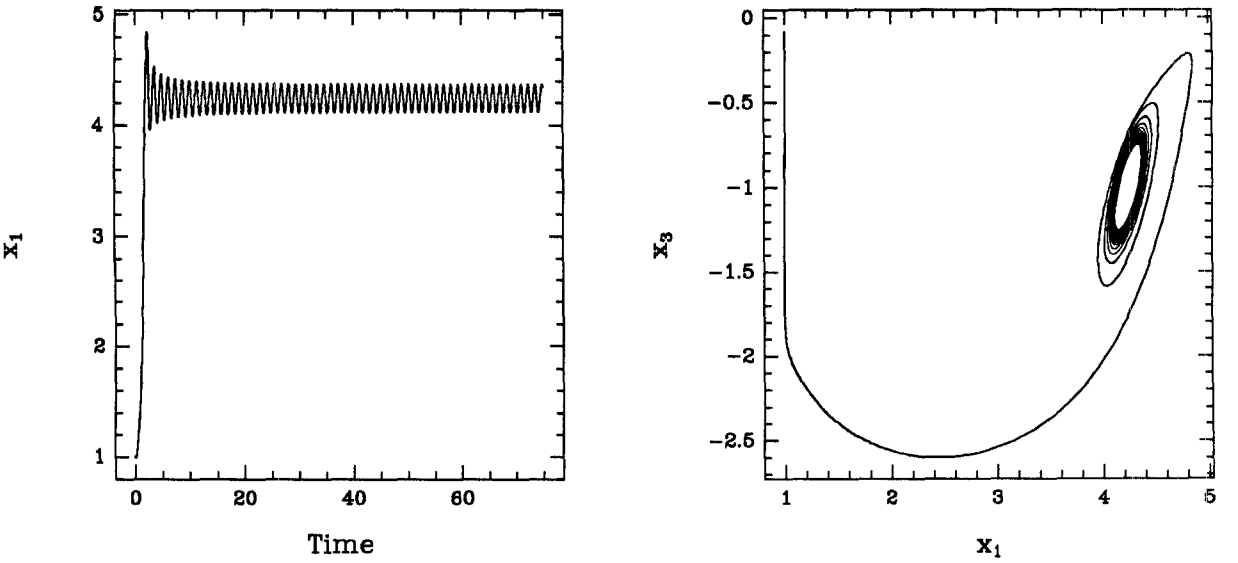

(a) (b)

Figure 9: A trajectory of closed loop system under nonlinear 'stabilizing' control with $k_n = 2.5$ for $R = 19$

Ruelle-Takens route to chaos in systems with dimension greater than three. The effect of transferring between different chaos scenarios is also an interesting subject.

4.3 Delaying and Stabilizing the Hopf Bifurcations

As shown in the previous subsections, a linear feedback control can be used to delay the Hopf bifurcations and a nonlinear one can be employed to stabilize the Hopf bifurcations. The linear feedback control is only effective to a limited extent in suppressing chaos. The nonlinear control, on the other hand, is very effective in suppressing chaos without affecting the linear stability of the original system. However, the linear feedback does increase the stability margin of the steady convective equilibria. Thus a natural extension to the control laws above is a combined linear-plus-nonlinear feedback control. The linear part of the feedback is chosen to delay the Hopf bifurcations to a desired value of R, and the nonlinear part of the feedback is chosen to stabilize the Hopf bifurcations occurring in the closed loop

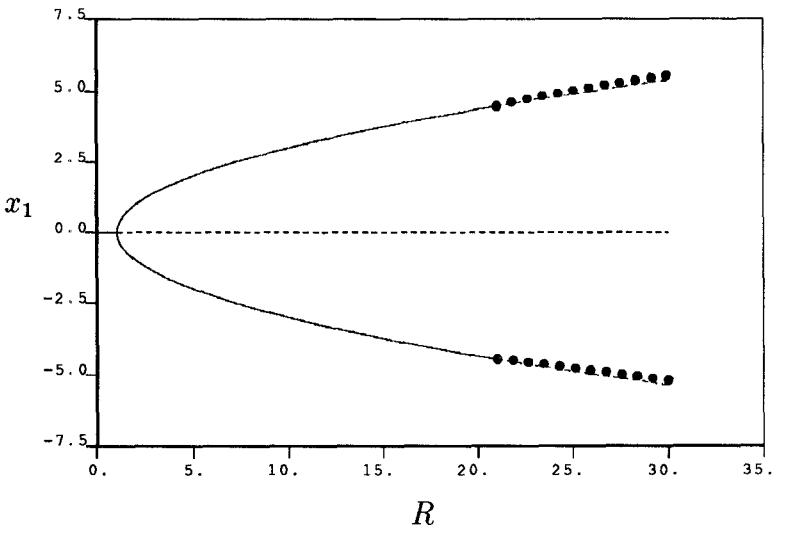

Figure 10: Bifurcation diagram for linear-plus-nonlinear control with $k_l = 0.182538$ and $k_n = 2.5$

system. Again choosing the simplest such control laws, the closed loop system takes the form (20)-(25), except that now the controller is

$$u = -k_l y - k_n y^3. \tag{32}$$

The control can be designed in two stages. In the first stage, adjustment of k_l is used to delay the parameter value at which the Hopf bifurcations occur to an acceptable value. In the second stage, k_n is adjusted to stabilize the Hopf bifurcation points and the bifurcated periodic solutions resulting from the Hopf bifurcations. Figure 10 shows a bifurcation diagram of the closed loop system with one such linear-plus-nonlinear feedback control. Note that the control law (32) effects both a delay in the occurrence of the Hopf bifurcations, and stabilization of these bifurcations.

With this type of control, both transient chaos and chaos are successfully suppressed. The linear component in the control allows one to have control of the stability margin of the steady convective equilibria. The nonlinear term in the control not only stabilizes the Hopf bifurcations but also removes the periodic orbits windows. Thus one expects a significantly improved transient response of the system than that achieved using linear feedback alone.

So far all the proposed control approaches preserve the "symmetry" of the system because of the way the control is introduced. Only the asymmetric component x_3 of the states is used in constructing washout filters and controllers. This results in identical control action for the upper and lower equilibrium branches. The two Hopf bifurcations (upper branch and lower branch respectively) are relocated and/or stabilized in unison and the resulting stable convective equilibria and/or the stable limit cycles coexist, each with its respective basin.

Surely these approaches are very effective to relocate or suppress chaos, but for a given initial condition it is not very clear beforehand to which convective equilibrium or limit cycle the trajectory converges. It may be desirable not only to suppress chaos but also to be able to direct a trajectory to the neighborhood of a specified equilibrium. This motivates the design of another class of controllers, which imparts preference for one equilibrium over another. This is the subject of the next subsection.

4.4 Targeting Control

We now carry out the design of control laws to "target" a particular equilibrium of the system. That is, other equilibria or periodic orbits surrounding them are rendered unstable, while the target equilibrium, or a periodic orbit surrounding it, is stabilized. This is achieved by using the readily observable symmetric component x_2 of the state vector in constructing the controllers. A linear feedback is employed to increase the stability margin of one convective equilibrium and at the same time to decrease that of another convective equilibrium. A pure nonlinear feedback, on the other hand, is designed to stabilize the Hopf bifurcation of one equilibrium branch, leaving the linear stability of the original system and the stability of the other Hopf bifurcation unchanged. As in the case of the symmetry preserving control laws in the previous subsections, one can employ a combined linear-plus-nonlinear feedback approach to achieve other more flexible types of stability.

Targeting an Equilibrium Recall that the convective equilibria $C_{\pm}$ lose their stability at Hopf bifurcations occurring at $R = 16$. In Subsection 4.1, a linear feedback control is employed to modify the critical value of R at which *both* the Hopf bifurcations occur. Here,

we give controllers which result in changing the critical value of R to two different values for the C_+ branch and the C_- branch respectively. In other words, while the critical value of R at which the Hopf bifurcation associated with the C_+ (C_-) branch occurs is modified to a larger value of R, the critical value of R associated with the C_- (C_+) branch is modified to a lesser value of R. In doing so, the stability margin of one equilibrium is increased while that of the other is decreased. Hence, one equilibrium is preferred to the other ("targeted").

A linear washout filter aided feedback with measurement of x_2 is a dynamic feedback. The state variable x_2 is readily measurable. The closed loop system is given by

$$\dot{x}_1 = -px_1 + px_2, \tag{33}$$

$$\dot{x}_2 = -x_1x_3 - x_2, \tag{34}$$

$$\dot{x}_3 = x_1x_2 - x_3 - R + u, \tag{35}$$

$$\dot{x}_4 = x_2 - dx_4, \tag{36}$$

where the x_4 is the washout filter state, and where the control u takes the form

$$u = k_l y, \tag{37}$$

with y an output variable, given by

$$y := x_2 - dx_4, . \tag{38}$$

Here, k_l is a scalar (linear) feedback gain.

The control does not preserve the symmetry inherent in the model (1)-(3), though it does preserve the (symmetric) equilibrium structure of (1)-(3). However, the closed loop system (33)-(38) possesses symmetry involving the control gain k_l. That is, replacing (x_1, x_2, x_3, x_4) and k_l with $(-x_1, -x_2, x_3, -x_4)$ and $-k_l$, respectively, results in the same set of equations. Thus, the sign of k_l alone determines which equilibrium is stabilized. The effect of positive k_l on the system is opposite to that of negative of k_l. This can also be seen from the characteristic polynomials evaluated at C_+ and C_-. For positive (negative) k_l the stability margin of C_+ (C_-) is increased in the parameter space and that of C_- (C_+) is decreased.

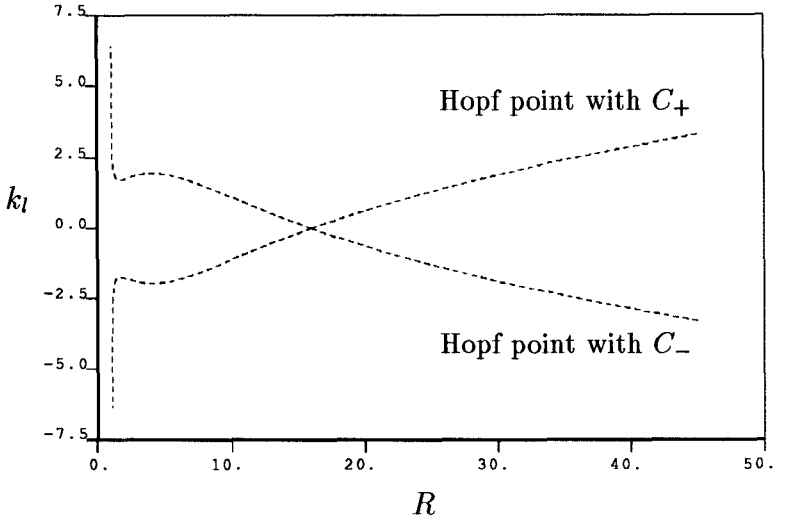

Figure 11: Two-parameter curves of Hopf bifurcation points for linear 'targeting' control

Figure 11 illustrates the 2-parameter (k_l and R) curves of the Hopf bifurcation points, i.e., the relationship between k_l and the critical values of R at which the Hopf bifurcations occur. Figure 12 shows a bifurcation diagram of the closed loop system for $k_l = 2.5$. It can be seen that C_+ is rendered stable up to $R = 36.0043$, and C_- is unstable for $R > 1.08538$. In the interval $1.08538 < R < 36.0043$, C_+ is stable and C_- is unstable. Hence typical system trajectories converge to C_+. Also note that the Hopf bifurcation at $R = 36.0043$ is still subcritical, while the Hopf bifurcation at $R = 1.08538$ is rendered supercritical. Switching the sign of k_l, say, $k_l = -2.5$, the situation is reversed: C_- is rendered stable in the same interval. So by reversing the sign of k_l one can switch the asymptotic behavior of the system from one equilibrium to another.

The relationship between k_l and the critical values of R at which the Hopf bifurcations occur is quantified by the conditions

$$\begin{aligned}&(-2p + dp + k_l p\sqrt{R-1} + dR + 2pR)^2 + (2dpR - 2dp)(2 + d + p)^2 \\ &-(2d + p + dp + k_l\sqrt{R-1} + R)(-2p + dp \\ &+ k_l p\sqrt{R-1} + dR + 2pR)(2 + d + p) = 0, \end{aligned} \tag{39}$$

$$-2p + dp + k_l p\sqrt{R-1} + dR + 2pR > 0, \quad \text{and} \quad R > 1. \tag{40}$$

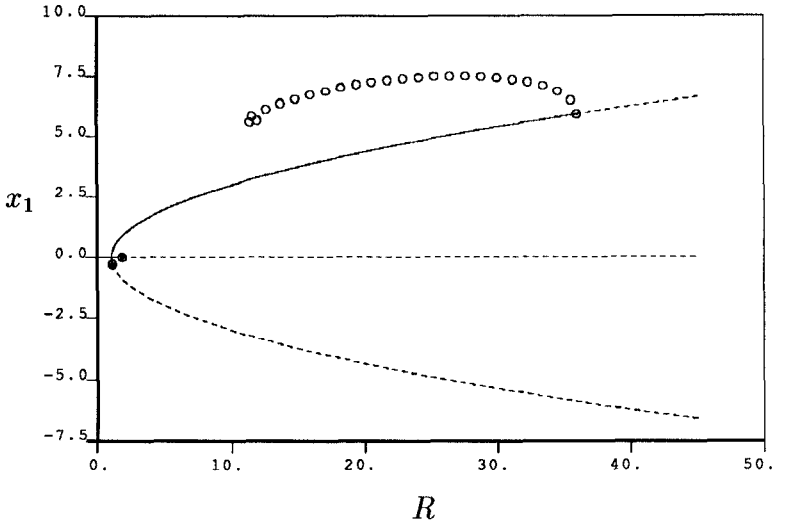

Figure 12: Bifurcation diagram for linear 'targeting' control with $k_l = 2.5$

Simulation evidence suggests that for some choices of k_l there are further bifurcations involving periodic orbits even for moderate values of R. (Recall that the open loop system as well as the closed loop with a linear feedback delaying Hopf bifurcations also experience bifurcations involving periodic orbits for some larger values of R.) However, simulations also suggest that for $|k_l| \leq 2.5$, such bifurcations are unlikely to occur. This in turn limits the ability of the proposed control to modify the critical values of R, therefore the ability to affect the stability margin of $C_{\pm}$. One way to accommodate this limitation is to apply a control strategy that combines the Hopf bifurcation delaying control and the targeting control discussed here. The presence of these 'unwelcome' bifurcations of periodic orbits signals the need for caution in applying linear control. Moreover, the closed loop system incorporating the control laws given above still exhibits chaotic and transient chaotic behavior. This chaotic (and transient chaotic) behavior is delayed to greater values of R. Also the chaotic (and transient chaotic) trajectories tend to spend more time around the preferred equilibrium. Next, we present a nonlinear feedback control which not only suppresses chaos but also targets a periodic orbit in the vicinity of a given equilibrium.

Before proceeding to issues of nonlinear control design, we again remark that the control introduced in the foregoing does not affect the stability of the nominal equilibrium branch,

i.e., the $(0, 0, -R, 0)$ branch. This is easy to verify by examing the associated characteristic polynomial.

Targeting the Vicinity of an Equilibrium In Subsection 4.1 a nonlinear dynamic feedback is designed to stabilize the Hopf bifurcations and the resulting closed loop system shows no chaotic behavior. In the previously chaotic region, two stable small amplitude periodic orbits coexist. Here we employ a similar type of nonlinear feedback but with the goal of introducing only one of these two periodic orbits. That is, one periodic orbit is rendered unstable, while a stable periodic orbit is introduced near the targeted equilibrium. This is achieved by stabilizing the Hopf bifurcation of one equilibrium branch, while not affecting the linear stability of the original system and the stability of the other Hopf bifurcation.

Using the bifurcation control techniques of Section 3, one can again show that there is a family of stabilizing, purely cubic nonlinear controllers. With the simplest such control law, the closed loop system again takes the form (33)- (38), except that now the controller is

$$u = k_n y^3. \tag{41}$$

Here, as before, k_n denotes a scalar (nonlinear) feedback gain.

Applying the Hopf bifurcation formulae (18) and (19) to the Hopf bifurcation associated with C_+ at $R = 16$, we find

$$\beta_2^* = \beta_2 - 0.35291 k_n. \tag{42}$$

For the Hopf bifurcation associated with C_-, we have

$$\beta_2^* = \beta_2 + 0.35291 k_n. \tag{43}$$

Recall that $\beta_2 = 0.02027 \pm 0.001087$.

Again one can see that the sign of k_n can be used for switching between the equilibria (actually, between periodic orbits in their vicinity). Also for $k_n > 0.06233$, the control $u = k_n y^3$ is a stabilizing control for the Hopf bifurcation associated with C_+. For $k_n < -0.06233$ the control u stabilizes the Hopf bifurcation associated with C_-. By changing the sign of k_n one can switch the asymptotic behavior of the system from one periodic orbit

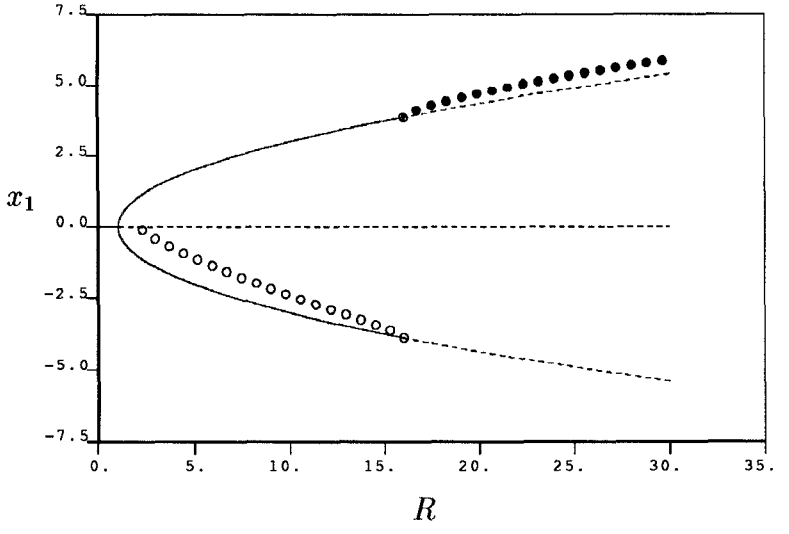

Figure 13: Bifurcation diagram for nonlinear 'targeting' control with $k_n = 2.5$

to another. These are local results. Bifurcation analysis and simulation evidence indicate that larger values of $|k_n|$ increase the stability margin in parameter space and also ensure a smaller amplitude of the periodic orbits. Figure 13 shows a bifurcation diagram of the closed loop system with $k_n = 2.5$. Note that the Hopf bifurcation point as well as the bifurcated periodic solutions associated with C_+ are stabilized while those associated with C_- are rendered unstable.

From a stability point of view, this approach results in the system preferring one periodic orbit to another. However, simulations show that though chaos is no longer present, the domain of attraction of the preferred (targeted) periodic orbit is not the whole space. Although one might hope that all trajectories of the closed loop system converge to the preferred period orbit (the only attractor), simulations indicate that some trajectories diverge to infinity. The stable manifold of the nominal saddle equilibrium separates the domains of attraction for the target periodic orbit and infinity. In the closed loop system, even the stable convective equilibrium for which the associated Hopf bifurcation is still subcritical has its domain of attraction significantly reduced as compared with the case for the open loop system. These undesirable effects can, fortunately, be circumvented by the scheme described next. This scheme is basically the same as that used by [3], except that in [3] linearization

and pole placement are employed.

Define a neighborhood $D(C_{\pm}, \epsilon)$ around C_+ or C_-. The neighborhood D can be of any shape, e.g., a ball. Denote ϵ the minimum distance from the points on the boundary of D to $C_{\pm}$. The size of D can be changed by adjusting ϵ. Now suppose the target periodic orbit is near C_+, i.e., the objective is such that for almost all initial conditions in the basin of the chaotic attractor, the dynamics of the system converges to the desired periodic orbit surrounding C_+. Continue to use the nonlinear control function (41). However, activate the control only if a trajectory from any given initial condition reaches D. Usually the trajectory is locked onto the desired attractor. In case the trajectory does wonder away from D, then deactivate the control and wait for the trajectory to enter D again. The ergodic nature of the chaotic dynamics ensures that the state trajectory eventually enters into this neighborhood. A typical trajectory experiences a chaotic transient. This may prove to be undesirable in some cases. Again, by switching the control, i.e., the sign of k_n we can switch the system dynamics from one periodic orbit to another one.

Let us conclude this section with some remarks on the relationship among the various controllers presented. First, note that linear feedback and nonlinear feedback are presented separately in this subsection. However, they may be combined to yield a controller of the form $u = k_l y + k_n y^3$ which introduces further freedom in the achievable dynamical structure of the system and its limit sets. Moreover, one can also combine the targeting control results of the current subsection with control laws for delaying bifurcations and those for stabilizing bifurcations presented in previous subsections. In general, these control laws illustrate how the bifurcation control approach may be employed to yield various stability goals related to the bifurcations displayed by a given system, without modifying its equilibrium structure.

5 Conclusions

Using bifurcation control ideas, control laws have been systematically designed for the suppression of both transient chaotic and chaotic motion in a thermal convection system model.

The control laws exactly preserve all the equilibrium branches of the system, and can be designed to simultaneously stabilize *both* convective equilibrium branches. This stabilization can take one of two forms. One can literally stabilize the equilibria using linear dynamic feedback. But the closed loop system can still exhibit transient chaotic and chaotic motion for some value (larger) of the Rayleigh number R due to bifurcations of periodic orbits. Alternatively, it is possible to re-locate the Hopf bifurcations to occur at higher values of the Rayleigh number R, and then employ nonlinear control to ensure stability of these bifurcations. In this way, a small amplitude stable limit cycle is introduced which surrounds the equilibrium for parameter values at which it is unstable. Simulations show that this control scheme is effective in suppressing chaos for any parameter range. For some parameter ranges the choice between linear feedback and linear-plus-nonlinear feedback depends on several factors, including degree of confidence in the model and available net gain. However, both types of feedback are related in their structure, especially in their incorporation of washout filters and preservation of model symmetry. Other controllers are also designed so that in addition to the goal of taming chaos, one can "target" a particular equilibrium or its vicinity. That is, other equilibria or periodic orbits are rendered unstable, while the target equilibrium or periodic orbit is stabilized. By changing the signs of the controllers, one can switch the asymptotic behavior of the system from one equilibrium or periodic orbit to another.

Although this paper has focused on a particular model with particular set of bifurcations, the approach itself may be viewed in the following general terms. Design of feedback control laws directed at primary bifurcations in a succession of bifurcations leading to chaos is a viable technique for the taming of chaos. Chaos can be suppressed, relocated in parameter and state space, and its type may be changed. Moreover, this can be achieved in a robust fashion, maintaining the positions of system equilibria even in the presence of model uncertainty. The resulting controllers do not depend on the bifurcation parameter and are effective over a range of parameter values.

Acknowledgment

This research has been supported in part by the National Science Foundation's Engineering Research Centers Program: NSFD CDR-88-03012, by NSF Grant ECS-86-57561, by the Air Force Office of Scientific Research under URI Grant AFOSR-87-0073, and by the TRW Foundation.

References

[1] J. Singer, Y.Z. Wang & H.H. Bau, "Controlling a chaotic system," *Physical Review Letters* 66 (1991), 1123–1125.

[2] E. Ott, C. Grebogi & J.A. Yorke, "Controlling chaos," *Physical Review Letters* 64 (1990), 1196–1199.

[3] F.J. Romeiras, E. Ott, C. Grebogi & W.P. Dayawansa, "Controlling chaotic dynamical systems," *Proc. 1991 American Control Conference*, Boston (1991).

[4] T.B. Fowler, "Application of stochastic control techniques to chaotic nonlinear systems," *IEEE Trans. Automatic Control* AC-34 (1989), 201–205.

[5] T.L. Vincent & J. Yu, "Control of a chaotic system," *Dynamics and Control* 1 (1991), 35–52.

[6] A. Hübler, "Adaptive control of chaotic systems," *Helvetica Physica Acta* 62 (1989), 343–346.

[7] A.I. Mees, *Dynamics of Feedback Systems*, Wiley, New York, 1981.

[8] J. Baillieul, R.W. Brockett & R.B. Washburn, "Chaotic motion in nonlinear feedback systems," *IEEE Trans. Circuits and Systems* CAS-27 (1980), 990–997.

[9] R. Genesio & A. Tesi, "Harmonic balance methods for the analysis of chaotic dynamics in nonlinear systems," *Automatica* (to appear).

[10] H.C. Lee & E.H. Abed, "Washout filters in the bifurcation control of high alpha flight dynamics," *Proc. 1991 American Control Conference*, Boston (June 1991).

[11] C. Sparrow, *The Lorenz Equations: Bifurcations, Chaos, and Strange Attractors*, Springer-Verlag, New York, 1982.

[12] E.A. Jackson, *Perspectives of Nonlinear Dynamics* #2, Cambridge Univ. Press, Cambridge, 1990.

[13] J. Singer & H.H. Bau, "Active control of convection," *Phys. Fluids A* 3 (1991), 2859–2865.

[14] Y. Wang, J. Singer & H.H. Bau, "Controlling chaos in a thermal convection loop," *J. Fluid Mechanics* 237 (1992), 479–498.

[15] E.H. Abed & J.H. Fu, "Local feedback stabilization and bifurcation control, I. Hopf bifurcation," *Systems and Control Letters* 7 (1986), 11–17.

[16] H.C. Lee, "Robust Control of Bifurcating Nonlinear Systems with Applications," University of Maryland, College Park, Ph.D. Dissertation, 1991.

[17] E.J. Doedel, "AUTO: A program for the automatic bifurcation analysis of autonomous systems," *Cong. Num.* 30 (1981), 265–284.

[18] J.M.T. Thompson & H.B. Stewart, *Nonlinear Dynamics and Chaos*, Wiley, Chichester, 1986.

[19] L.P. Sil'nikov, "A case of the existence of a denumerable set of periodic motions," *Soviet Math. Dokl.* 6 (1965), 163–166.

[20] B.D. Hassard, N.D. Kazarinoff & Y.H. Wan, *Theory and Applications of Hopf Bifurcation*, Cambridge Univ. Press, Cambridge, 1981.

[21] J.E. Marsden & M. McCracken, *The Hopf Bifurcation and Its Applications*, Springer-Verlag, New York, 1976.

[22] T. Kailath, *Linear Systems*, Prentice-Hall, Englewood Cliffs, NJ, 1980.